



HAL
open science

Ianos-A Hurricane in the Mediterranean

K. Lagouvardos, A. Karagiannidis, S. Dafis, A. Kalimeris, V. Kotroni

► **To cite this version:**

K. Lagouvardos, A. Karagiannidis, S. Dafis, A. Kalimeris, V. Kotroni. Ianos-A Hurricane in the Mediterranean. *Bulletin of the American Meteorological Society*, 2022, 103, pp.E1621-E1636. 10.1175/BAMS-D-20-0274.1 . insu-03778111

HAL Id: insu-03778111

<https://insu.hal.science/insu-03778111>

Submitted on 23 Feb 2023

HAL is a multi-disciplinary open access archive for the deposit and dissemination of scientific research documents, whether they are published or not. The documents may come from teaching and research institutions in France or abroad, or from public or private research centers.

L'archive ouverte pluridisciplinaire **HAL**, est destinée au dépôt et à la diffusion de documents scientifiques de niveau recherche, publiés ou non, émanant des établissements d'enseignement et de recherche français ou étrangers, des laboratoires publics ou privés.

Ianos—A Hurricane in the Mediterranean

K. Lagouvardos, A. Karagiannidis, S. Dafis, A. Kalimeris, and V. Kotroni

ABSTRACT: During 15–21 September 2020, an intense medicane, named Ianos, formed over the warm Mediterranean Sea. Following a path of approximately 1,900 km, Medicane Ianos affected Greece resulting in four casualties and devastating damage in the western and central parts of Greece. Persistent gale force 1-min winds up to 44 m s^{-1} and wind gusts up to 54 m s^{-1} were recorded in Cephalonia Island (Ionian Sea), while record-breaking amounts of accumulated rainfall have been recorded in several Ionian islands, as well as in parts of central Greece. Analysis of the available observations showed that Ianos was the most intense medicane ever recorded in the Mediterranean. This paper aims at investigating the genesis and evolution of the medicane, based on in situ observations, satellite measurements, and model analyses. Toward that objective, Meteosat Second Generation (MSG) SEVIRI imagery, combined with lightning data permitted to follow the evolution of convective activity during the various phases of Ianos. This investigation is complemented with upper-air model analyses in order to evaluate the synoptic environment within which Ianos had formed and was sustained over 7 days. Finally, the Global Precipitation Measurement *Core Observatory* (GPM *CO*) satellite overpasses over Medicane Ianos provided invaluable information about its 3D structure, especially during its most intense phase.

KEYWORDS: Cyclogenesis/cyclolysis; Dynamics; Hurricanes/typhoons; Extreme events

<https://doi.org/10.1175/BAMS-D-20-0274.1>

Corresponding author: Dr. Kostas Lagouvardos, lagouvar@noa.gr

Supplemental material: <https://doi.org/10.1175/BAMS-D-20-0274.2>

In final form 16 September 2021

©2022 American Meteorological Society

For information regarding reuse of this content and general copyright information, consult the [AMS Copyright Policy](#).

AFFILIATIONS: Lagouvardos, Karagiannidis, and Kotroni—Institute for Environmental Research, National Observatory of Athens, Athens, Greece; Dafis—Institute for Environmental Research, National Observatory of Athens, Athens, Greece, and LMD/IPSL, CNRS UMR 8539, École Polytechnique, Université Paris Saclay, ENS, PSL Research University, Sorbonne Universités, UPMC Univ. Paris 06, Palaiseau, France; Kalimeris—Laboratory of Environmental Physics, Energy, and Environmental Biology, Department of Environment, Ionian University, Zakynthos, Greece

The Mediterranean Sea occasionally hosts intense cyclones with characteristics similar to tropical cyclones, such as a frontless and axisymmetric structure, deep convection close to their centers with a windless “eye” and sustained wind speeds close to hurricane strength (Lagouvardos et al. 1999). Such cyclones are often named “medicanes.” Although most of their lifetime is spent over the sea, when they reach the coasts of Mediterranean countries they can be very destructive. Recent case studies have investigated the formation and intensification mechanisms of these cyclones, which are mainly attributed to baroclinic processes (e.g., Mazza et al. 2017; Fita and Flaounas 2018) and to intense surface fluxes (Miglietta and Rotunno 2019). Noyelle et al. (2019) suggested that the higher the sea surface temperature (SST) during a medicane, the higher is the probability for tropical transition and thermodynamic intensification of the medicane, similarly to tropical cyclones. Thus, in a warming climate there is a special concern about the future changes of medicanes’ intensity and frequency of occurrence, with several independent studies showing an increasing trend of stronger medicanes in the near future (e.g., González-Alemán et al. 2019; Koseki et al. 2020).

Between 2016 and 2020, four strong medicanes have developed in the Ionian Sea (Dafis et al. 2020) and have caused damage in Greece, with the most recent and most destructive case being the Medicane Ianos between 15 and 20 September 2020. In October 2016, Medicane Trixie battered the south coasts of Greece with excessive rainfall up to 180 mm in less than 12 h in Crete and wind gusts stronger than 30 m s^{-1} . One year later, in November 2017, Medicane Numa hit the west coasts of Greece resulting in severe flooding, landslides, and excessive precipitation. Medicane Zorbas in September 2018 was one of the costliest weather-related disaster in Greece in the past decade, bringing hurricane-force wind speeds in south Greece and causing severe flooding in central Greece (up to 506 mm of rainfall in 48 h).

Ianos initially emerged as a surface cyclone close to a thunderstorm cluster in the Gulf of Sidra on 15 September 2020, off the coasts of Libya (Fig. 1). Global and regional model guidance showed a highly possible transition of the surface cyclone to a powerful medicane, a fact that led the METEO unit at the National Observatory of Athens (NOA) to name the medicane “Ianos” in the morning of 16 September, following NOA’s practice adopted since 2017 to name weather events that are expected to produce high socioeconomic impacts (www.meteo.gr/namedstorms.cfm). Based on satellite imagery [namely, on Spinning Enhanced Visible and Infrared Imager (SEVIRI) imagery, various scatterometers’ data, and Global Precipitation Measurement *Core Observatory* (GPM CO) data], Ianos was evolved into a powerful medicane on 17 September 2020 when it started gradually to affect Greece with storm surges accompanied by high coastal waves, high rainfall amounts, and devastating winds, which resulted in four fatalities and extended infrastructure damages and landslides in the Ionian Islands and in central Greece. Zekkos et al. (2020) reported that the torrential rainfall resulted

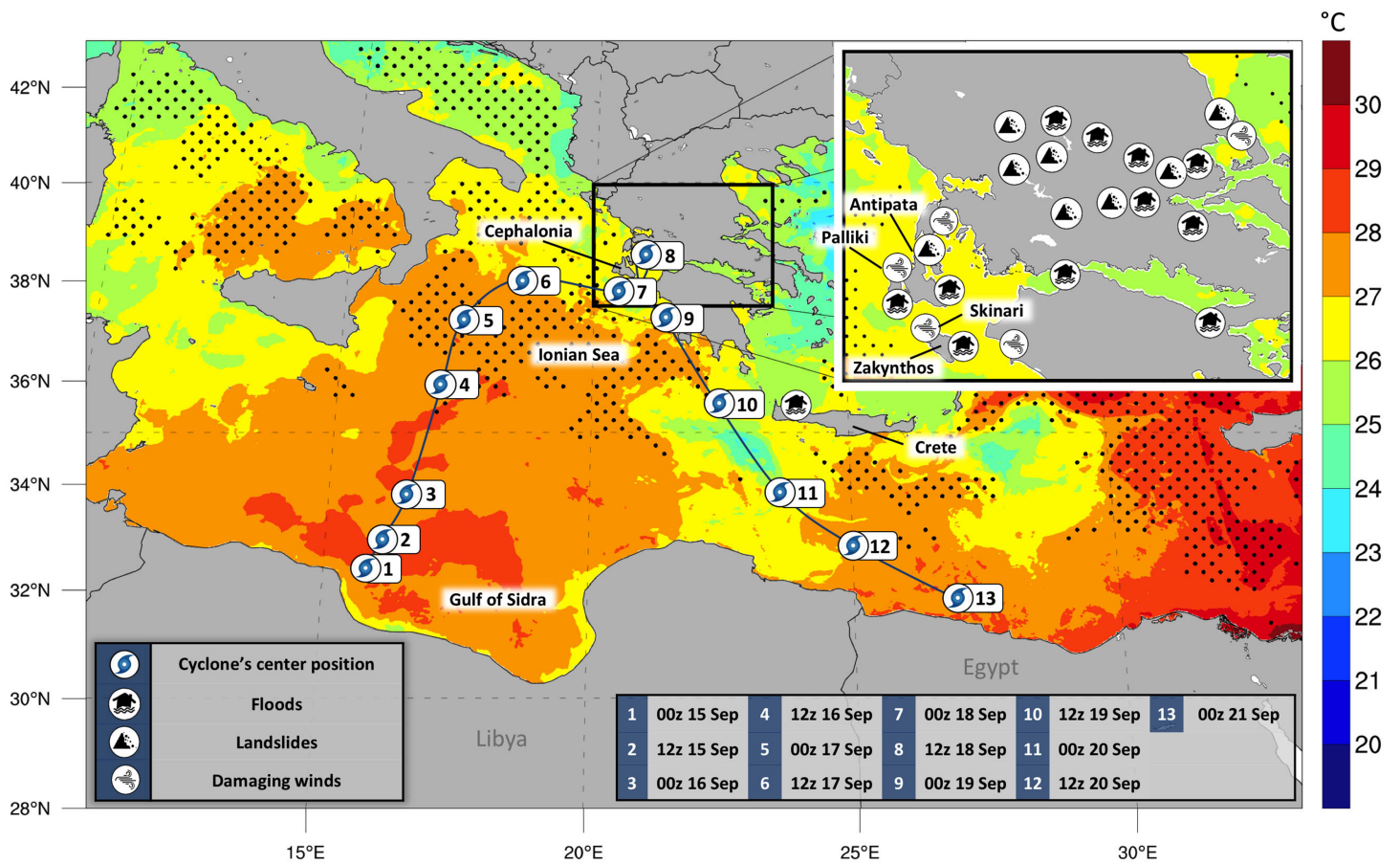


Fig. 1. Path of Medicane Ianos, from 0000 UTC 15 Sep up to 0000 UTC 21 Sep 2020. Shading denotes the SST (at 1-K intervals), and the black dots the daily SST anomaly higher than 2 K on 15 Sep 2020. Symbols for floods, landslides, and damaging winds are placed over the most affected areas.

in a large number of landslides and debris flows and more specifically in central Greece the authors mapped more than 1,400 landslides in 2 days.

The objective of this study is to highlight important aspects of the development of this high-impact medicane based on the analysis of the available in situ and satellite observations along with model-derived fields aiming to better understand its formation and evolution mechanisms. The physical processes behind the formation and behavior of medicanes have been intensively studied during the last decade (e.g., Tous and Romero 2013; Picornell et al. 2014; Fita and Flaounas 2018). As the observational and modeling tools are continuously updated and improved, the scientific community is able to utilize new information toward improved understanding of medicanes. Based on previous studies regarding the intensity and impact of medicanes (Winstanley 1970; Miglietta et al. 2013, their Table 1; Cioni et al. 2016; Dafis et al. 2020, their supporting information S1), our analysis offers insights into the formation and evolution on the strongest medicane ever recorded. The main novel element of the present work is the use of the state-of-the-art observational tools (like the GPM CO Microwave Imager and the Dual-Frequency Precipitation Radar), which can be used to analyze the convective nature of Medicane Ianos in high detail. A secondary, yet important, novelty is the fact that it is actually the first time that GPM CO captures a medicane in its mature state, allowing us to observe its shape, cloud bands, and precipitation regime at that stage. The added value of the analysis is mostly the new information gained from these observations, which can definitely improve our knowledge and help us prepare against and mitigate the effects of such high-impact weather phenomena.

Data and tools

The METEO unit at NOA operates the NOAA network of 430 automatic surface weather stations in Greece that is monitoring all basic meteorological variables at 10-min intervals (Lagouvardos et al. 2017). Due to the absence of a homogenized operating weather radar network, the weather station network allowed the real-time monitoring and analysis of the spatiotemporal distribution of rainfall produced by Ianos. Moreover, an additional local network that covers the Ionian Islands (Kalimeris et al. 2015) provided higher temporal resolution (at 1-min intervals) weather observations of Ianos's core.

The synoptic conditions during the event were investigated using the Final Operational Global Analysis of the National Centers for Environmental Prediction (NCEP FNL). FNL analyses are available at $0.25^\circ \times 0.25^\circ$ spatial and 6-h temporal resolution. Meteosat Second Generation (MSG) SEVIRI brightness temperatures on water vapor at the $6.2\text{-}\mu\text{m}$ (WV6.2) channel and infrared at the $10.8\text{-}\mu\text{m}$ (IR10.8) channel together with lightning data provided by ZEUS very low-frequency (VLF) lightning detection network (Kotroni and Lagouvardos 2016) permitted to construct the full path of Ianos as well as to scrutinize its convective nature.

GPM, initiated by NASA and the Japan Aerospace Exploration Agency (JAXA) as a global successor to TRMM, comprises a consortium of international space agencies (e.g., CNES, ISRO, NOAA, EUMETSAT). It consists of a constellation of research and operational satellites, where the NASA/JAXA GPM CO satellite, carrying the radar/radiometer, serves as a reference standard to unify precipitation measurements. The GPM CO encompasses a multichannel conical-scanning microwave imager—the GPM Microwave Imager (GMI) (Draper et al. 2015) and a Dual-Frequency Precipitation Radar (DPR) (Kojima et al. 2012). GMI has 13 microwave channels that measure brightness temperature (Tb) sensitive to precipitation type ranging from light to heavy rain, snow, and ice. The reader can find information about the GMI channels in Hou et al. (2014). DPR consists of a Ku- and a Ka-band-frequency radar and can offer 3D data of precipitation particles inside the cloud systems. Overpasses of the GPM CO satellite provided invaluable data of the 3D structure of Ianos during its mature stage.

Path of Medicane Ianos—In situ rainfall and wind observations

The area of genesis of Medicane Ianos was over northern Libya and the surface cyclone could be first tracked by satellite imagery when it passed over the Gulf of Sidra, at the beginning of its 7-day-long life. Figure 1 shows Ianos's path between 15 and 21 September 2020, when, after a route of approximately 1,900 km, it made landfall in the Mediterranean coast of Egypt. This path was inferred by the combined analysis of sea level pressure (SLP) provided by FNL and tracking of the cyclonic curvature or the closed circular patterns of clouds based on MSG SEVIRI imagery. Ianos formed over the warm waters of the Gulf of Sidra, where SST exceeded 28°C (Fig. 1) based on satellite observations from the Ultra-High Resolution Sea Surface Temperature Analysis product (Buongiorno Nardelli et al. 2013). According to the daily SST climatology built from 21 years (1985–2005) of AVHRR Pathfinder data (Marullo et al. 2007), the SST anomaly in the Ionian Sea was higher than $+2\text{ K}$. Ianos acquired its tropical characteristics, like the symmetric frontless structure, over the anomalously warm Ionian Sea at around 0300 UTC 17 September 2020.

Luckily, Ianos' core was sampled by a weather station in Palliki, northwest Cephalonia (Fig. 1), while 4 weather stations recorded the evolution of surface pressure, 10-m wind, and rainfall within 50 km from Ianos's "eye." It is worth mentioning that such observations are very rare given the small size of medicanes. The previous most recent case when a medicane "eye" was sampled by surface stations was in 2014, in Malta during Medicane Qendresa (Cioni et al. 2018).

Hurricane-force winds, resulted in extended damage in the Ionian Islands (see Fig. 1 for the location of the most affected areas), fortunately with no loss of human lives. The minimum SLP of 984.3 hPa, as well the maximum wind speed and gust was recorded in Palliki, Cephalonia, when at the same time the weather station in Skinari, north Zakynthos, reported 989.1-hPa minimum SLP and 42.0 and 30.2 m s⁻¹ maximum 1-min wind gust and mean wind speed, respectively (Fig. 2). These extreme values took place a few hours after a sharp wind direction change during torrential rainfall inside Ianos’s “eyewall” cloud bands between 0000 and 0400 UTC 18 September 2020 (Fig. 2). The highest 1-min mean wind speed, derived by wind measurements at a sampling rate of 1 Hz, was 44.1 m s⁻¹ while the corresponding wind gust (maximum recorded wind speed over the same interval) was 54.2 m s⁻¹. When looking at the 10-min-average records, the corresponding highest values were 39.3 m s⁻¹ for the mean wind speed and 47.6 m s⁻¹ for the wind gust. In addition, the weather station in the northernmost part of Cephalonia in Antipata (Fig. 1) reported a record-breaking daily accumulated rainfall of 644.7 mm. These values are the highest ever recorded during a medicane and some of the highest ever recorded in Greece.

The rainfall distribution in Greece during the 48 h ending at 1200 UTC 19 September 2020 shows two distinct areas of maximum rainfall (Fig. 3a), one in the Ionian Islands

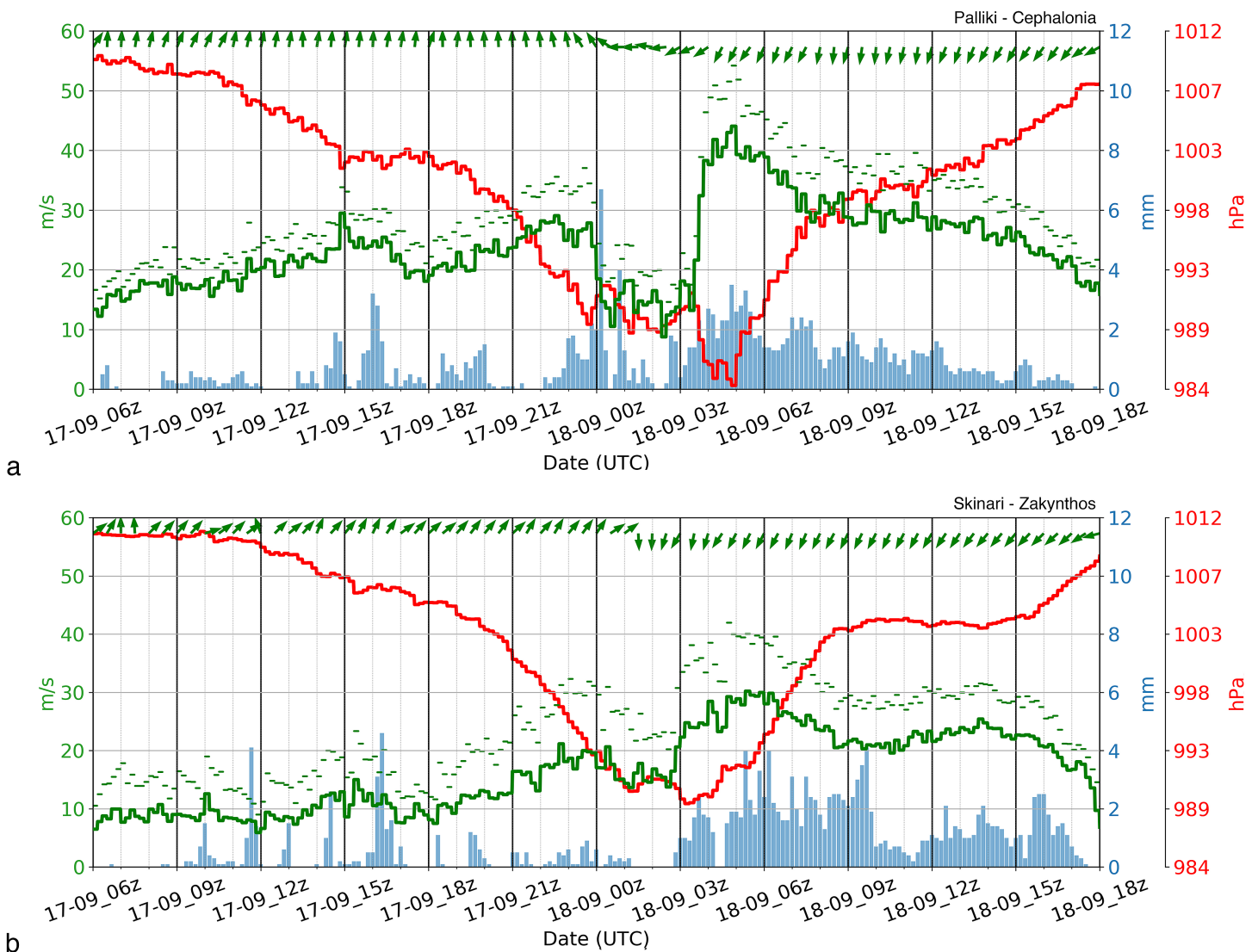


Fig. 2. Time series of mean sea level pressure, wind, and precipitation in (a) Palliki in Cephalonia and (b) Skinari in Zakynthos between 0600 UTC 17 Sep and 1800 UTC 18 Sep 2020: 10-min max 10-m wind speed (green line), max wind gust (green rectangles) (m s⁻¹), 30-min mean wind direction at 10-m height (green vectors), 10-min minimum sea level pressure (hPa; redline), and 10-min accumulated rainfall (blue bars; mm).

and one in central Greece (the latter detailed with a zoom in Fig. 3b). The 48-h (17 and 18 September 2020) accumulated rainfall in the Ionian Islands reached 769 and 250 mm in Cephalonia and Zakynthos Islands, respectively. During the same period, a very strong easterly flow was established over central Greece, associated with the low-level medicane flow in the Ionian Sea, which resulted in local strong low-level convergence zones and long-lasting rainfall with extreme rain rates. On 18 September 2020 the daily accumulated

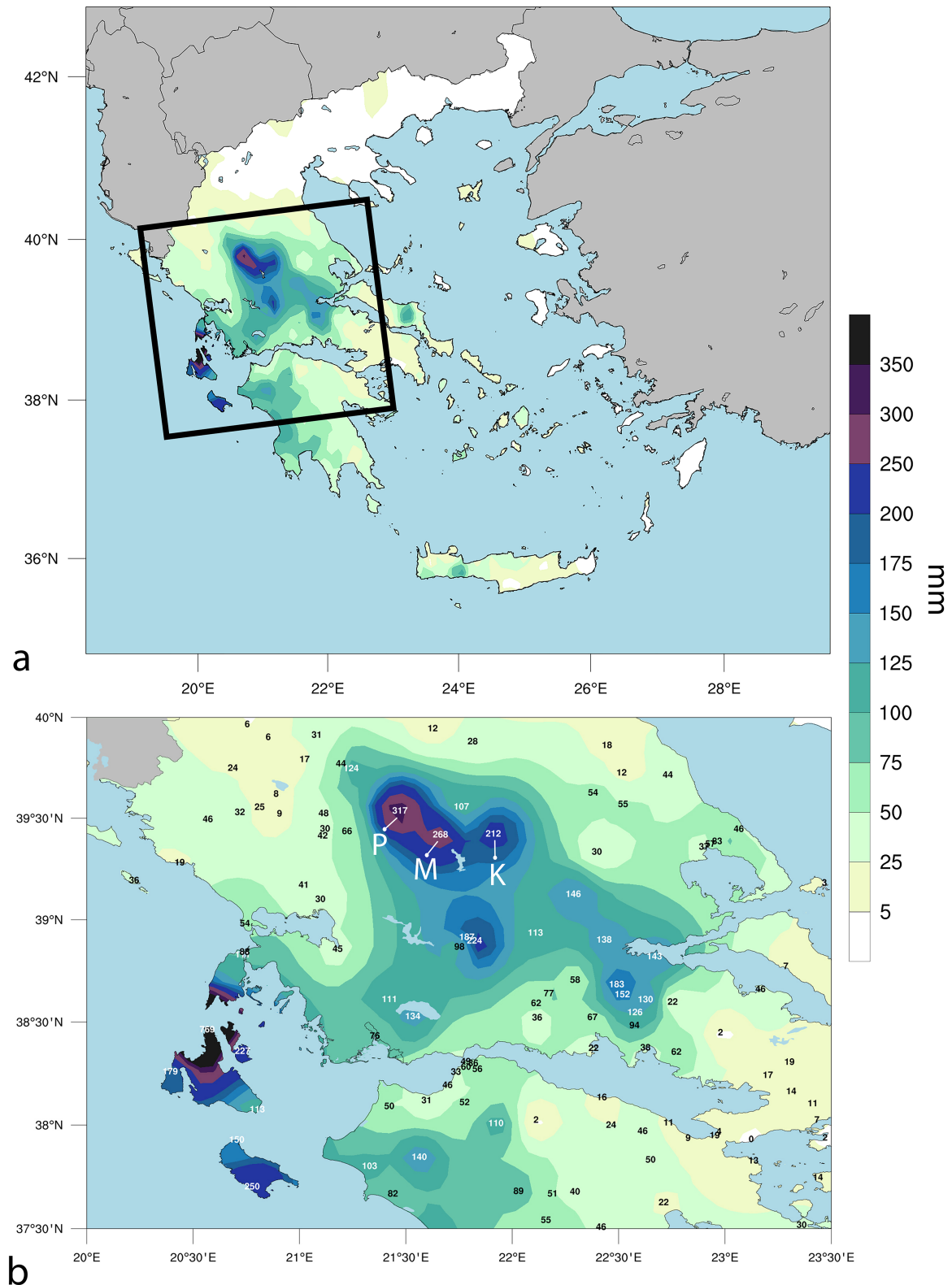


Fig. 3. (a) Total accumulated rainfall over Greece for the period spanning from 1200 UTC 17 Sep to 1200 UTC 19 Sep 2020 (48 h) and (b) zoom over central Greece, for the same period.

rainfall exceeded 250 mm in central Greece. The high amounts of precipitation in central Greece resulted in widespread flooding, extensive damage in rural and urban areas, and unfortunately four fatalities. Figure 3 shows the 48-h accumulated rainfall at the stations of Pertouli (P), Karditsa (K), and Mouzaki (M) in central Greece (see Fig. 3b for the location of the stations). The highest value was recorded in Pertouli (P), at the station located at the highest elevation among the three stations (1,170 m), with a total amount of 317 mm. Mouzaki (M) and Karditsa stations (K) recorded 268 and 212 mm of rain within the same time period.

Satellite imagery

Figure 4 provides four snapshots of MSG SEVIRI satellite infrared imagery (IR 10.8 μm) in the time period 16–18 September 2020. Infrared imagery is combined with the brightness temperature difference between the 6.2- μm water vapor and the 10.8- μm infrared channels, which can be used as an indication of convective activity (Olander and Velden 2009; Dafis et al. 2020).

At 1200 UTC 16 September 2020 (position 4 in Fig. 1) Ianos had not yet lost its extratropical characteristics, but it was characterized by high convective activity on the western flank of the cyclone center, as inferred by the close to zero and positive values of the WV–IR brightness temperature differences (Fig. 4a). The presence of convection is also supported by the

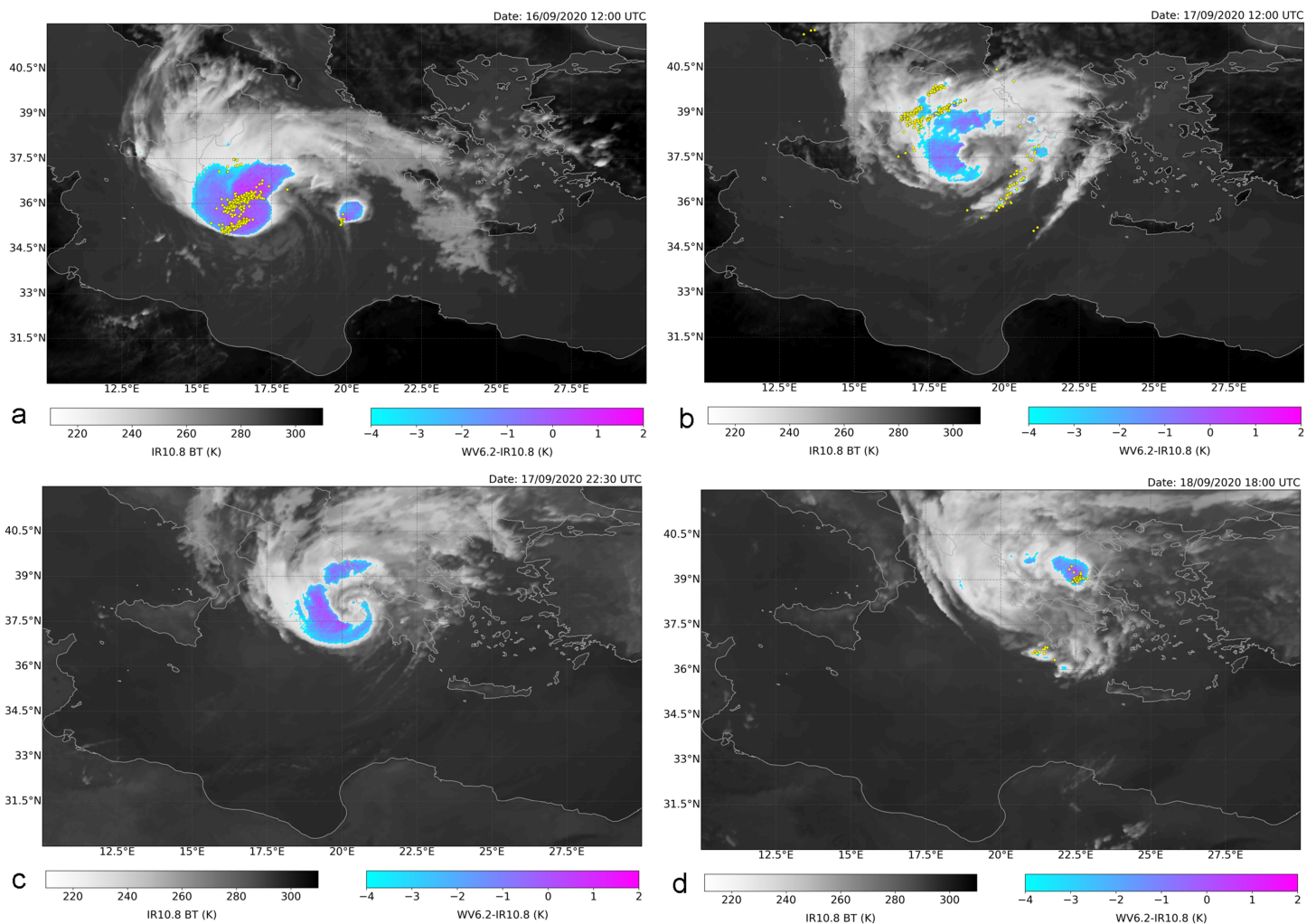


Fig. 4. MSG SEVIRI infrared brightness temperature (grayscale), and brightness temperature difference between the WV6.2 and IR10.8 channels (color scale), valid at (a) 1200 UTC 16 Sep, (b) 1200 UTC 17 Sep, (c) 2230 UTC 17 Sep, and (d) 1800 UTC 18 Sep 2020. Yellow dots denote lightning strikes detected by ZEUS network within 60 min before and after the satellite nominal time.

cloud-to-ground (CG) lightning activity observations, provided by ZEUS network (yellow marks in Fig. 4a).

The characteristic whirl of clouds is clearly observed 24 h later, at 1200 UTC 17 September 2020 (Fig. 4b). Convection is evident on the western flanks of the medicane (Fig. 4b), but it is slightly weaker than 24 h earlier. Lightning activity presents a wide spread around the vortex but now it is located farther away from the center.

At 2230 UTC 17 September (this instance was selected as it almost coincides with the GPM CO overpass discussed later in the “GPM measurements” section), the cloud walls around the center of the cyclone retain heights reaching the tropopause as suggested by the negative but close-to-zero or positive values of the WV–IR brightness temperature differences (Fig. 4c). Feidas and Giannakos (2011) state that positive or close-to-zero values of that difference indicate tall opaque clouds approaching or breaking the tropopause barrier. However, lightning activity in the specific instance is absent.

During the period of intense rainfall over central Greece, at 1800 UTC 18 September (Fig. 4d) Medicane Ianos has lost its symmetry and convection is limited mainly over parts of central Greece, with localized lightning activity. During the next 48 h, while Ianos was following a path toward Crete and the coasts of Egypt (see Fig. 1) it maintained a quasi-symmetric structure around its center, with scattered lightning activity, mostly far from its center. The full path of Ianos, as inferred by satellite imagery and concurrent lightning activity is provided in the online supplementary material (<https://doi.org/10.1175/BAMS-D-20-0274.2>).

Synoptic-scale setting of Ianos

The synoptic environment, into which Medicane Ianos formed over the Gulf of Sidra, was associated with a cutoff low dominating the central Mediterranean. The low is clearly identified at the 500-hPa level (Fig. 5a). At this stage (1200 UTC 16 September), as already stated, Ianos was not yet a medicane, as indicated by a pronounced vortex tilt, namely, the eastward shift of the surface low pressure center with respect to the center of the cutoff at 500 hPa. Twenty-four hours later, at 1200 UTC 17 September 2020, both low- and upper-level lows were vertically aligned, a typical synoptic pattern associated with a mature medicane (Fig. 4b). The same structure is evident at 2300 UTC 17 September, when Ianos’s center was offshore the coasts of western Greece (Fig. 4c), moving very slowly toward south (Fig. 5d). It should be noted, however, that due to its low spatial resolution, FNL analysis is not able to realistically depict the minimum sea level pressure values within Ianos’s center, which were recorded by the surface weather stations networks, discussed earlier in the “Path of Medicane Ianos—In situ rainfall and wind observations” section.

Analysis of the potential vorticity (PV) field at the 335-K isentropic level revealed that an upper-level intrusion of dry air of stratospheric origin approached the vortex at 1200 UTC 16 September. This PV streamer approached the area over the low center and wrapped around it (Fig. 6a). These upper-level disturbances set the precursor environment for the subsequent evolution of a cyclone and favor its intensification during the first phase of its formation (Cioni et al. 2016; Miglietta et al. 2017; Flaounas et al. 2020).

At 1200 UTC 17 September, Ianos was already a medicane and the PV structure presents the characteristic alignment throughout the troposphere, with the creation of a PV “tower” in the center of the medicane (Fig. 6b). It is worth mentioning that high upper-level PV values vanished near the area around the medicane center, due to the fact that a major part of it has been eroded at earlier stages by deep convection within the cloud bands around the medicane.

Inspection of the effective precipitable water (EPWAT) and integrated vapor transport fields indicate advection of moist air masses related to Ianos. The EPWAT is calculated by the subtraction between the FNL-derived precipitable water and the vertically integrated saturation deficit. Therefore, maps of EPWAT permit to identify the areas with the highest

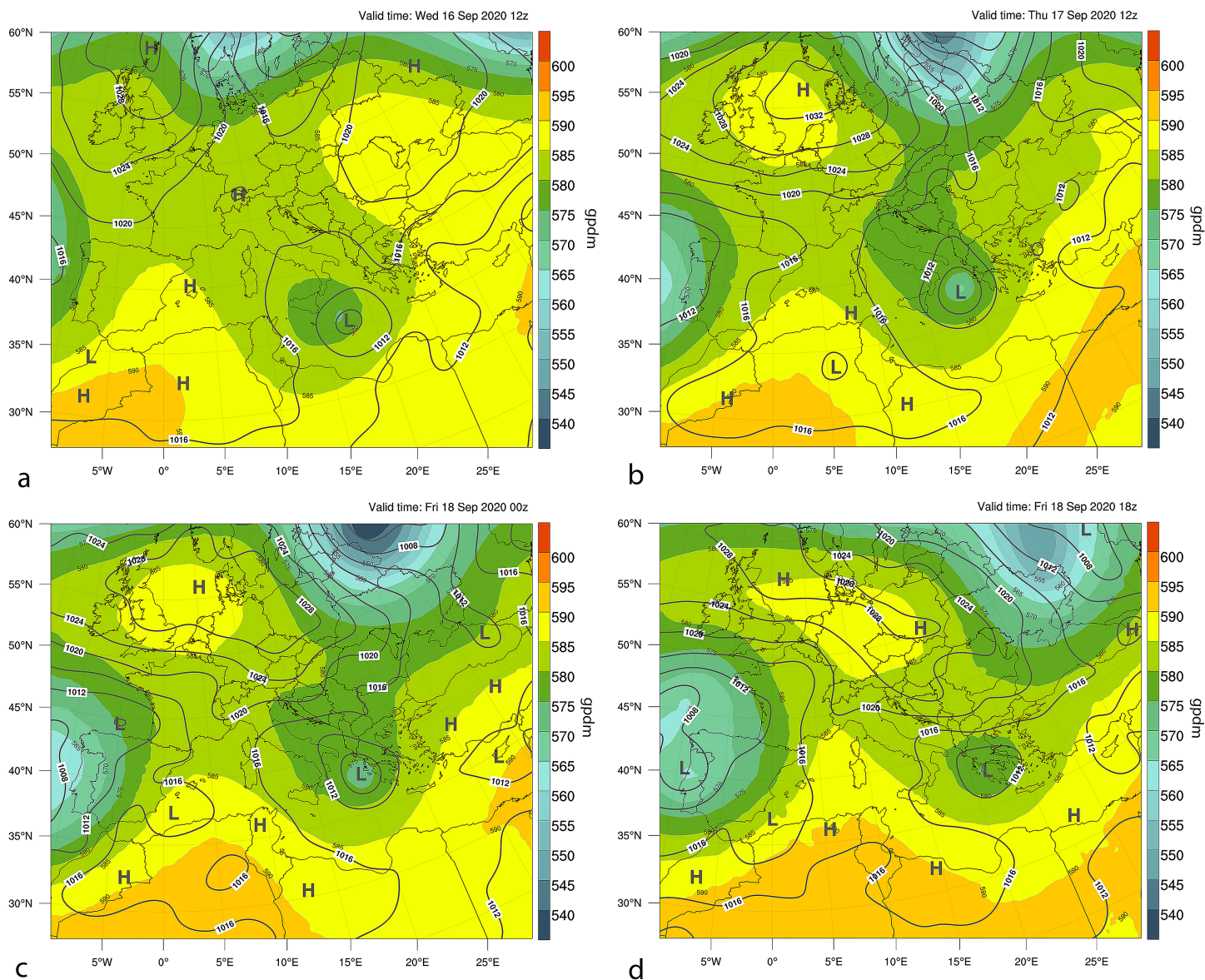


Fig. 5. NCEP FNL analysis of 500-hPa geopotential height (shading at 50-dam intervals) and sea level pressure (thin black contours at 2-hPa intervals), valid at (a) 1200 UTC 16 Sep, (b) 1200 UTC 17 Sep, (c) 0000 UTC 18 Sep, and (d) 1800 UTC 18 Sep 2020.

tropospheric moisture content that can lead to high rainfall amounts. During the lifetime of Ianos, extreme values of water vapor in the troposphere were transported from the south Ionian Sea toward continental Greece and high rainfall amounts were reported in many places. Figure 7 shows the integrated tropospheric water vapor transport as well as the EPWAT at the same four instances as in Fig. 5. According to these analyses, the EPWAT exceeded 50 mm offshore western Greece between 1200 UTC 17 September and 0000 UTC 18 September (Figs. 7b,c). A value of 50 mm is considered as extreme for the Mediterranean area while it is more common in the tropics (Sudradjat et al. 2005). In the evening hours of 18 September 2020 (Fig. 7d) high values of EPWAT are also evident over central Greece. During this time frame, the highest accumulated rainfall was recorded over this area, as discussed earlier in Fig. 3.

GPM measurements

GMI data. During the lifetime of Ianos, there were five overpasses of GMI covering the area of interest: at 1340 and 2320 UTC 16 September, 2230 UTC 17 September, 1240 UTC 19 September, and 2130 UTC 20 September 2020. Thus, the first two overpasses took place before Ianos entered its phase as a medicane (around 0300 UTC 17 September 2020) while

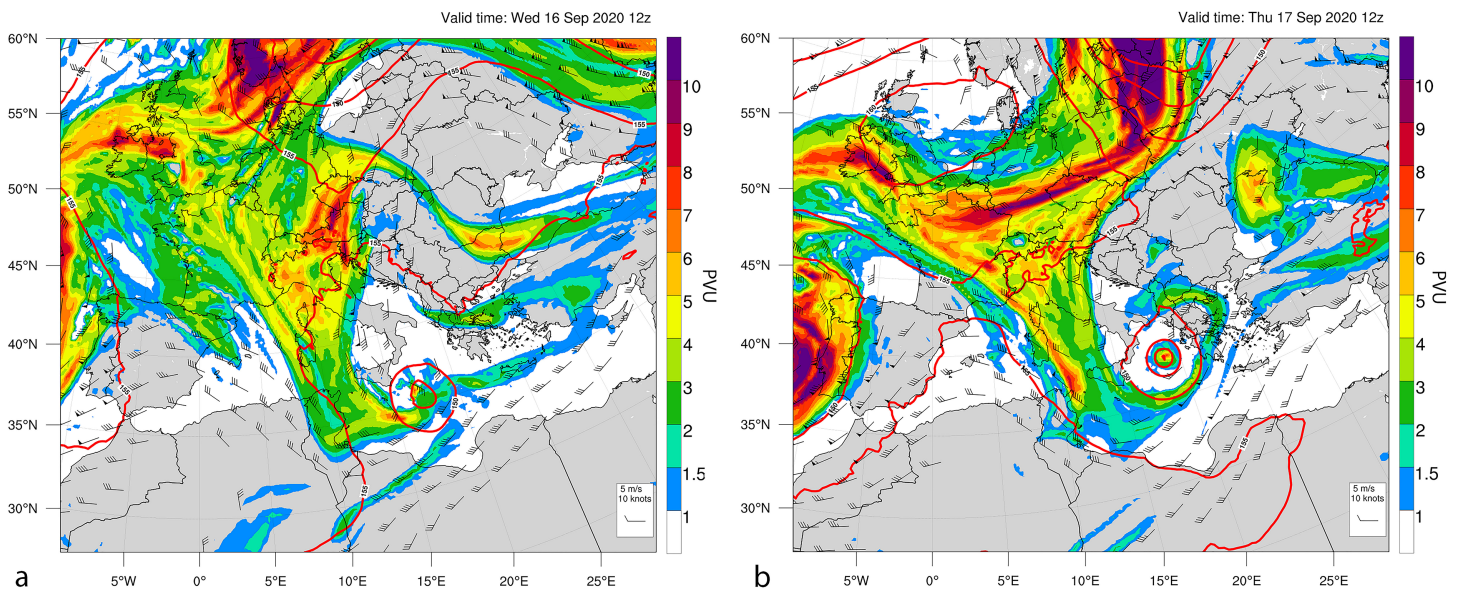


Fig. 6. Potential vorticity (shaded, PVU), wind barbs at the 335-K isentropic surface, and 850-hPa geopotential height (red contours, at 50-dam intervals), valid at (a) 1200 UTC 16 Sep and (b) 1200 UTC 17 Sep 2020.

the third overpass, when Ianos was an intense medicane, located very close to the western coast of Greece.

The vertically polarized at 89-GHz (V89 GHz) Tb imagery of GMI on 1340 UTC 16 September 2020 (Fig. 8a) shows a Tb decrease that reaches 129 K near the top of the cloud bands. Since that channel is strongly affected by ice and snow scattering, low Tbs indicate high amounts of frozen hydrometeors at the mid-/high levels of the troposphere, which are usually related to deep convective clouds and lightning. Indeed, lightning activity over the western flank of Ianos, as shown in Fig. 4a, was very high. High rainfall rates at the surface are indicated by the Tb increase in V10 GHz (Fig. 8b), a channel that is sensitive to radiative emission by liquid water. It should be noted, however, that lower-frequency channels suffer from lower spatial resolution (approximately 19 km \times 32 km for V10 GHz against 7 km \times 4 km for V89GHz) and therefore although they permit to follow the rainfall intensity changes during the medicane evolution, they do not provide details on the rainband structure within the medicane.

At 2320 UTC 16 September 2020, when Ianos was still in its development phase, a lower Tb depression (min Tb value = 163 K) on the cloud bands around the western flanks of the cyclone center is evident in the V89 GHz channel (Fig. 9a), suggesting weaker convective activity than 12 h earlier. Such a weakening of the convective activity before the TLC phase of a medicane has been identified and discussed in previous medicane studies, like the December 2005 case (Fita and Flaounas 2018; Dafis et al. 2020). This finding is also in agreement with ZEUS lightning observations that presented a significant decrease during the elapsed 12 h. The V10 GHz Tbs (Fig. 9b) is also lower around the cyclone center, a fact that supports a decrease of surface rainfall rates relatively to the previous GMI overpass.

Ianos became a powerful medicane around 0300 UTC 17 September. During the third GMI overpass over the area of interest, at 2230 UTC 17 September 2020, the cyclone center is found very close to the Ionian Islands. The V89 GHz channel (Fig. 10a) reveals a rotating pattern of ice hydrometeors around the center of the medicane, but V89 GHz Tb values are still higher and V10 GHz Tb values are still lower than the previous day (Fig. 8), indicating a gradual shift to a less convective status of the rainfall regime. As evidenced in the V10 GHz channel, the Tb increases close to the cyclone center (Fig. 10b), with respect to the previous overpass (Fig. 9b), providing thus a clear indication of persistent rainfall over the sea and the

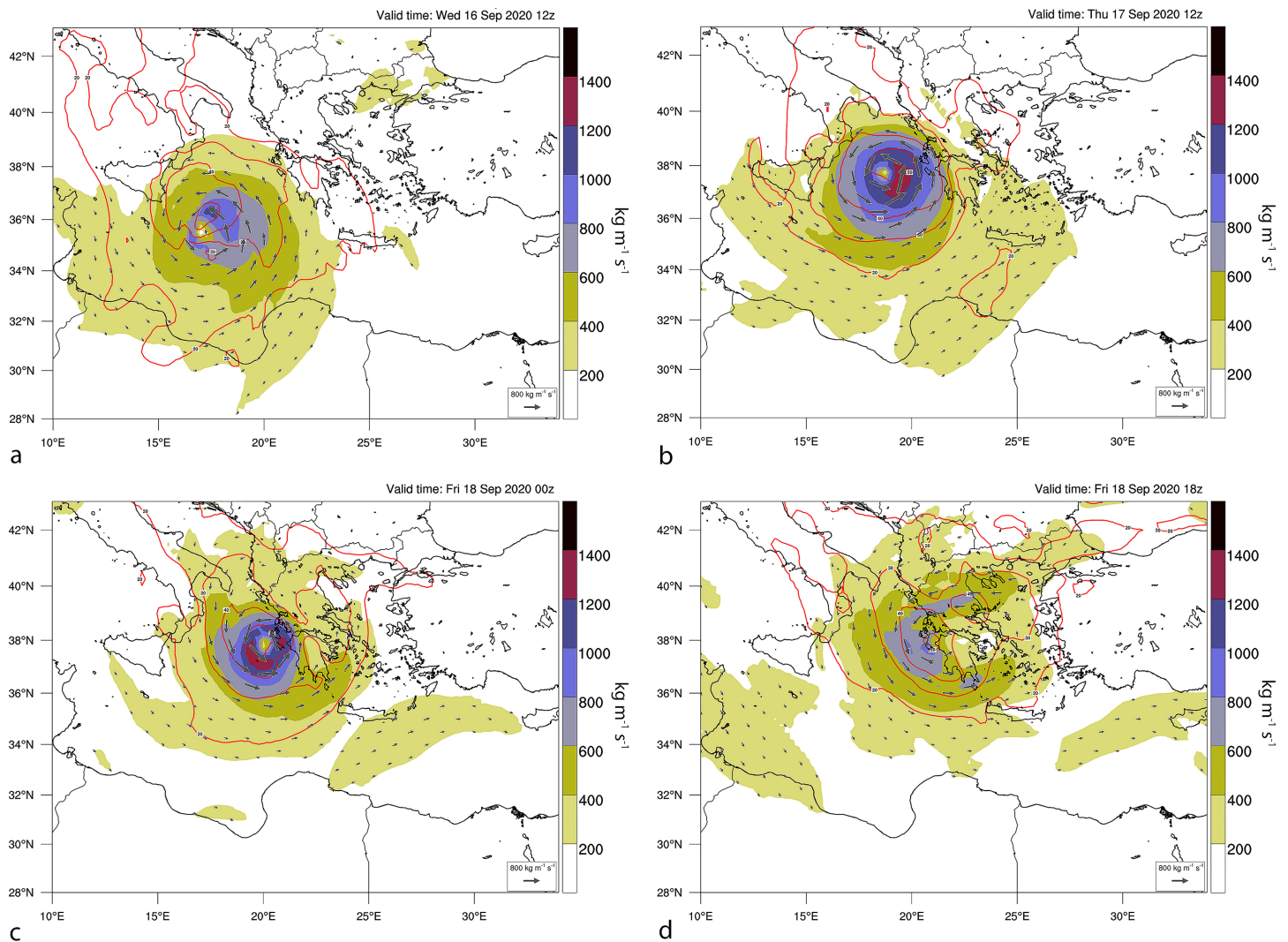


Fig. 7. Integrated tropospheric water vapor transport ($\text{kg m}^{-1} \text{s}^{-1}$, shading and arrows) and effective precipitable water (red contours with 10-mm intervals) at the same four times as in Fig. 5.

Ionian Islands. This finding is supported by the high EPWAT values that are provided by FNL (Fig. 7c) and the available rain gauge measurements.

It is worth noting that GPM CO overpasses over medicanes are very rare. Marra et al. (2019) presented an analysis of Medicanes Numa that also developed over the Ionian Sea between 15 and 19 November 2017 and affected southern Italy and Greece. The authors identified strong convective activity during the development phase of Numa and it was detected to be weaker after the maximum intensity of the cyclone. Concerning the Tb values in the V89 GHz channel, Marra et al. (2019) reported values as low as 158 K during the development stage of Medicanes Numa, a value substantially higher than the value of 129 K found over the western flank of Ianos during its developing stage (Fig. 8a). During the medicanes phase, Numa was showing only small portions of Tb depressions over its western flank (Marra et al. 2019, their Figs. 7 and 8), while Ianos showed large areas of Tb depressions over its western flanks, with no lightning activity, in contrast to its developing phase. Regarding the spatial distribution of convection, Ianos shares similarities with Medicanes Rolf (Dafis et al. 2018), Trixie, and Zorbas (Dafis et al. 2020) as convective activity was significantly reduced more than 150 km away from the medicanes center, but it was increased close to the core of the system within the first 50–100 km when the cyclone exhibited more symmetry and higher intensity. These results provide a different evolution for the distribution and intensity of convection with the three medicanes between 2003 and

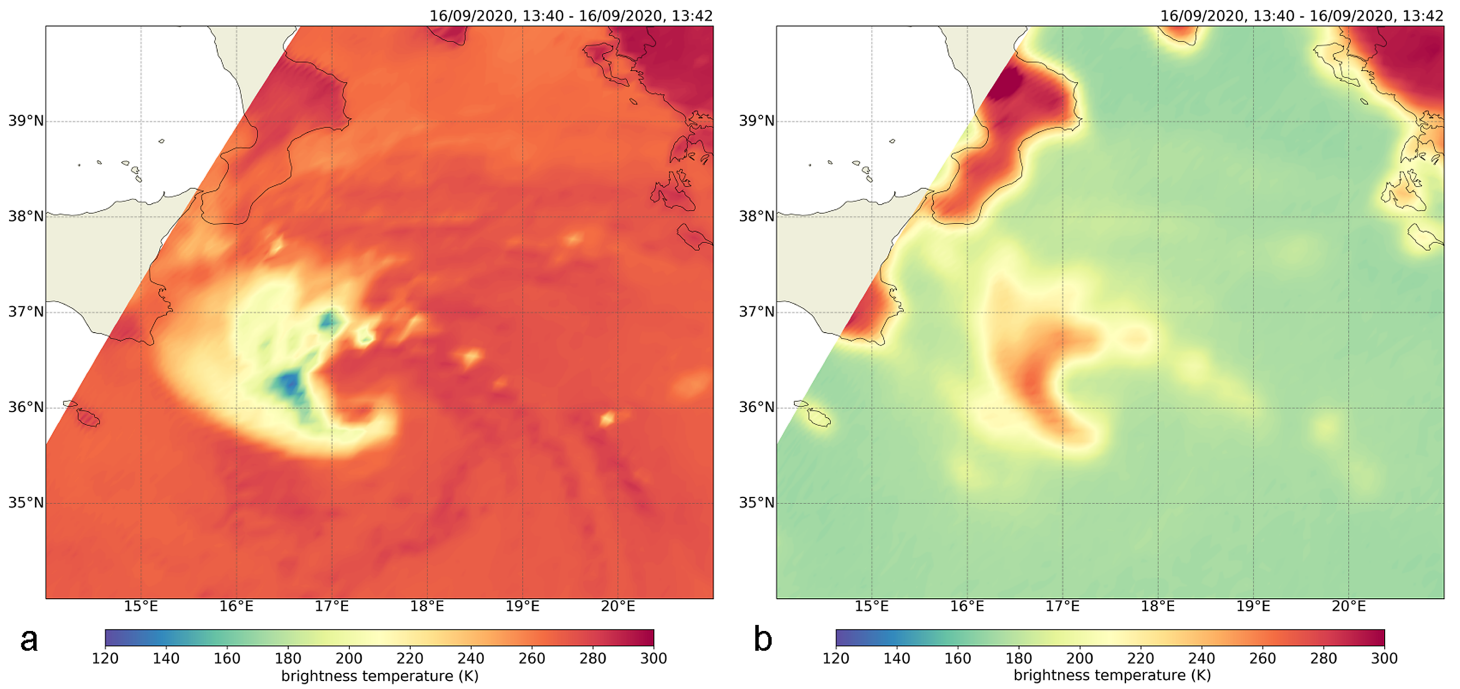


Fig. 8. GPM GMI brightness temperature (K) measured at (a) V89 GHz and (b) V10 GHz around 1340 UTC 16 Sep 2020.

2006 that were examined by Claud et al. (2010) and Miglietta et al. (2013), during which deep convection and precipitating clouds were not detected close to the center during the maximum cyclone intensity, despite the impressive cloud-free “eye” formation.

Precipitation Radar. The near-surface DPR corrected reflectivity (normal scan) at 2230 UTC 16 September 2020 is presented in Fig. 16, overlaid on the MSG SEVIRI infrared imagery (already shown in Fig. 4c). High reflectivity values dominate the ring around the medicane “eye,” with

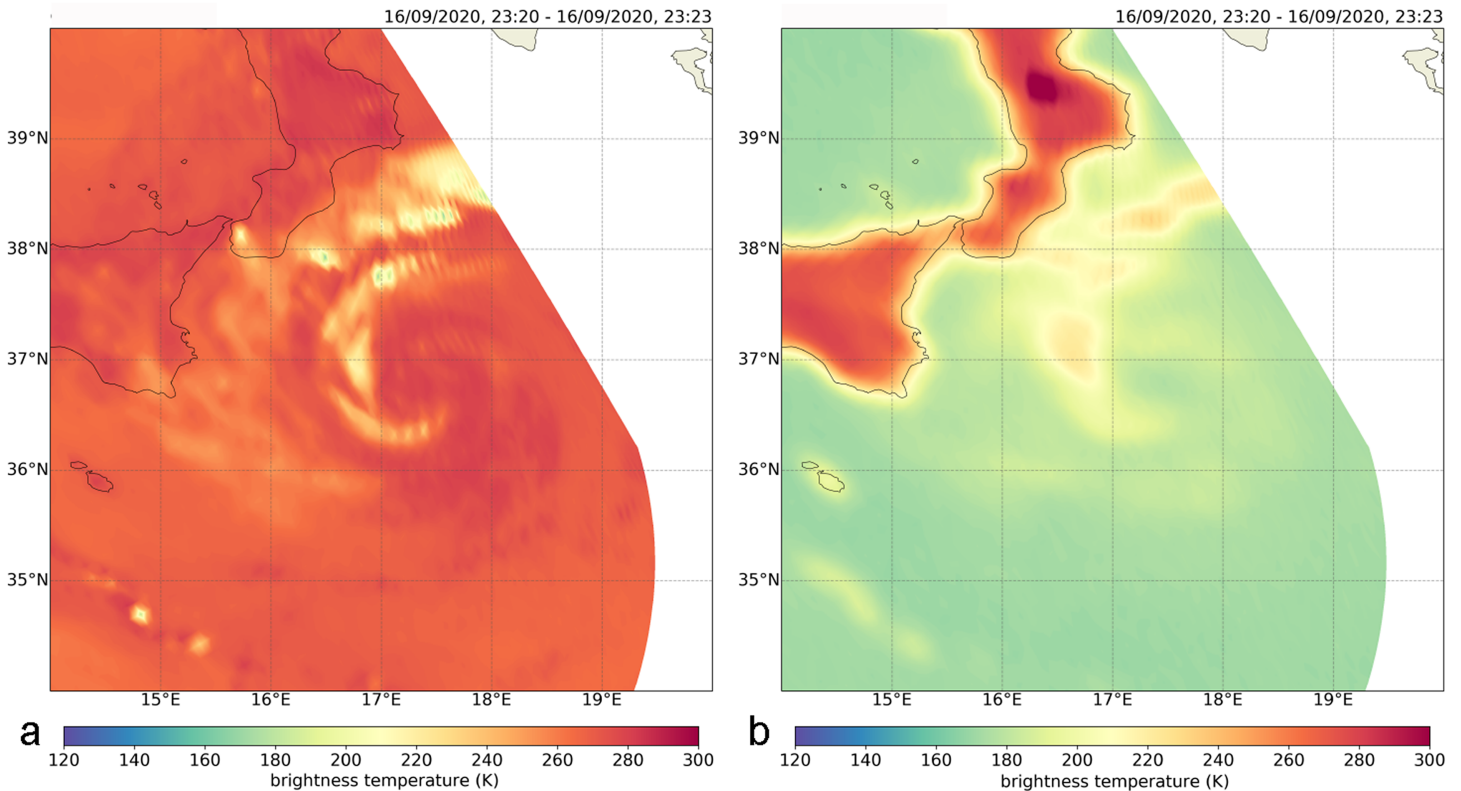


Fig. 9. GPM GMI brightness temperature (K) measured at (a) V89 GHz and (b) V10 GHz around 2320 UTC 16 Sep 2020.

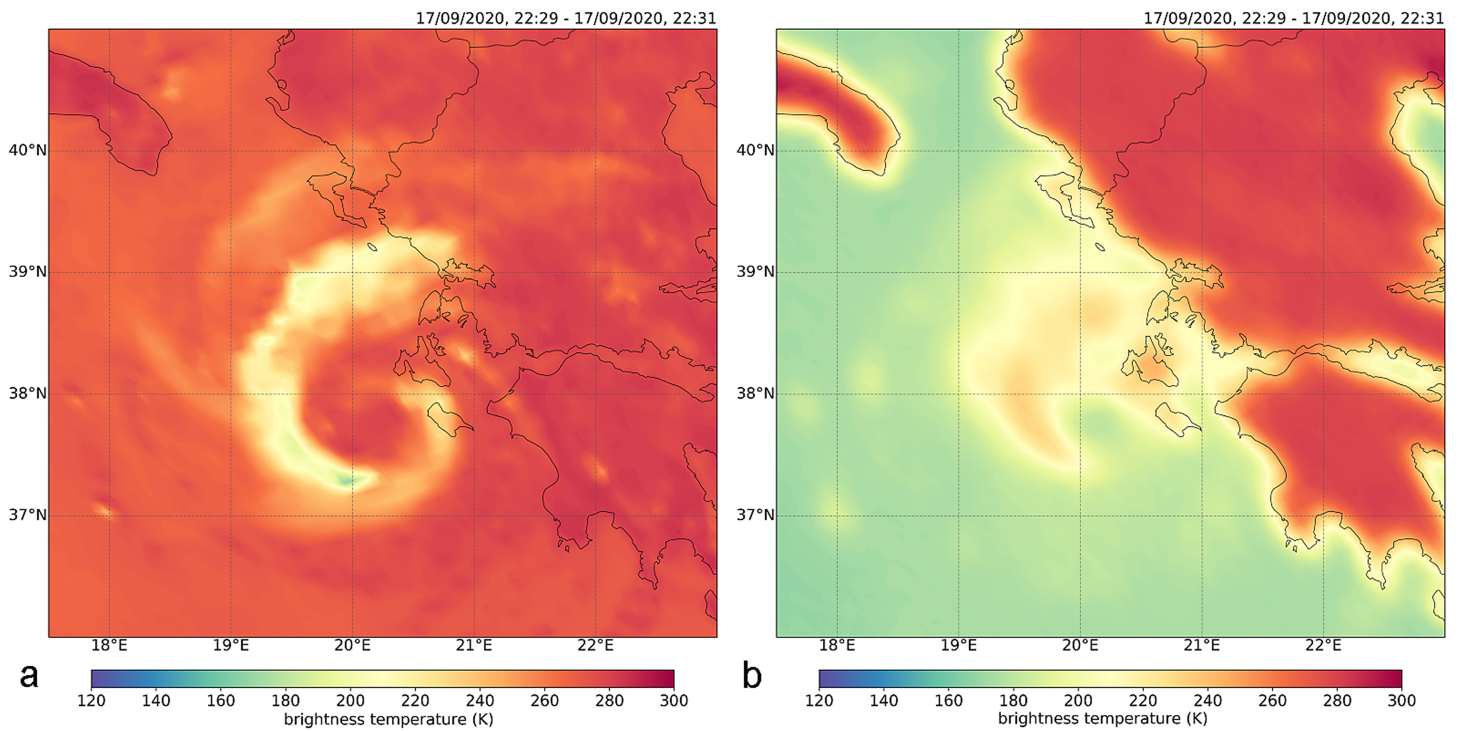


Fig. 10. GPM GMI brightness temperature (K) measured at (a) V89 GHz and (b) V10 GHz around 2230 UTC 17 Sep 2020.

the exception of the southeastern part of it. The spiral band around Ianos’s center is clearly evident and reminiscent of the cloud structures usually shown in tropical cyclones. The cloud-free area, the “eye” of Ianos, has a diameter of ~50 km, as inferred by the DPR measurements.

A 3D view of the reflectivity pattern associated to Ianos is shown in Fig. 12. The cloud bands around the eye are evident, while the surface of maximum height of the 20-dBZ reflectivity indicates the most vigorous cloud development over the southern flank of Ianos, reaching heights up to 11 km. This height is higher than the previous GPM DPR and ground-based radar

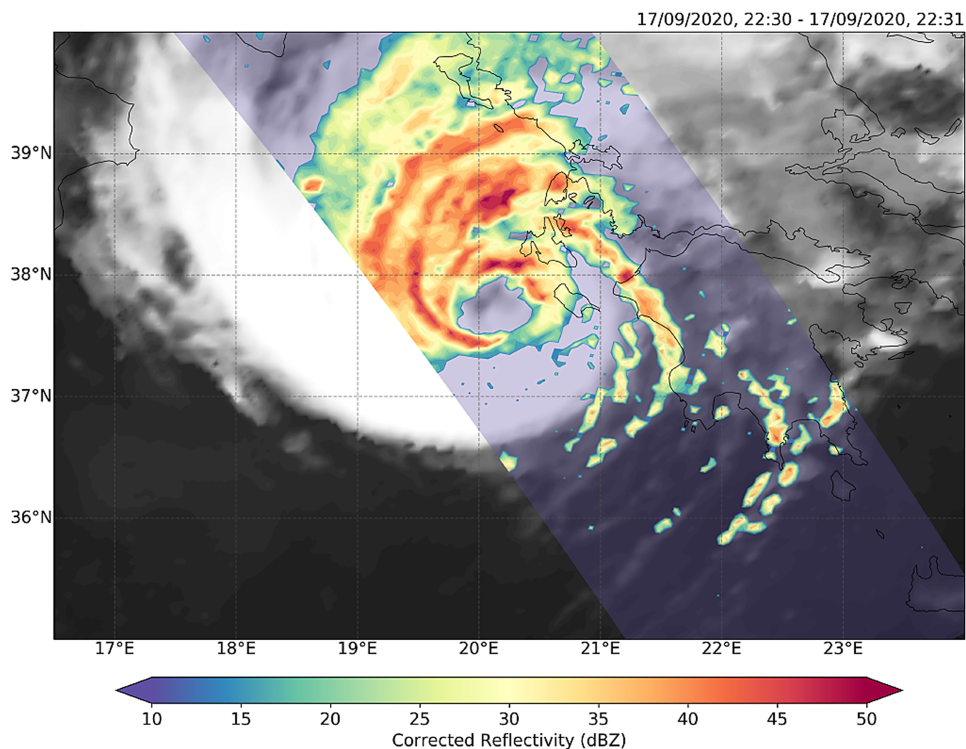


Fig. 11. GPM DPR near-surface corrected reflectivity (normal scan) around 2230 UTC 17 Sep 2020.

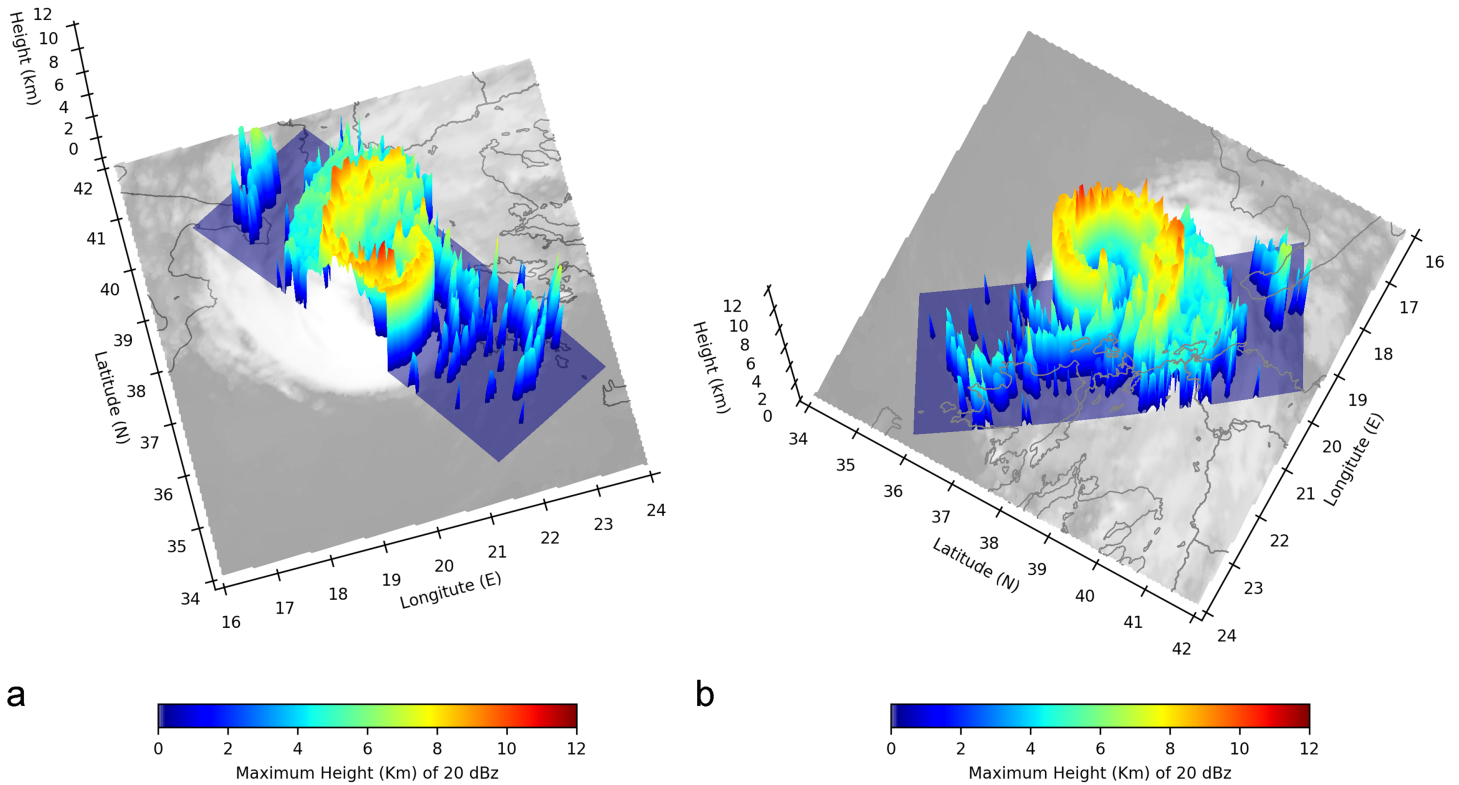


Fig. 12. GPM DPR maximum height of 20-dBZ reflectivity isosurface around 2230 UTC 17 Sep 2020 overlaid on MSG SEVIRI IR108 image: (a) view from southwest and (b) view from northeast.

measurements of Medicane Numa (Marra et al. 2019) when the cloud band tops were as high as 9–10 km. Within this rainband, reflectivity core of more than 45 dBZ was extending up to 5 km and the 20 dBZ isoline was found up to 10-km height, where close to zero and positive values of the WV–IR brightness temperature differences are found (see Fig. 4c). Interestingly, some of the highest values of corrected reflectivity in the northern flank of Ianos’s “eye” in Fig. 11 do not correspond to low T_b values in the V89 GHz channel (Fig. 10a). This can be partly explained by the data provided in Fig. 12, where high reflectivity values are confined in low altitudes in the troposphere, but these low-topped clouds were associated with torrential rainfall in the Ionian Islands as high precipitation rates were recorded during this period (not shown). Moreover V89 GHz is strongly affected by ice meteors that are mostly found in the middle and higher parts of troposphere, while Fig. 11 depicts near-surface reflectivity where the cloud bands are dominated by liquid water. A more detailed study would be needed to further explore the characteristics of these clouds around Ianos “eye” and their lack of lightning activity.

Concluding remarks

The analysis of all available in situ and satellite observations, of three GPM *CO* overpasses and of gridded analyses permitted to synthesize a coherent picture of Medicane Ianos during its entire lifetime. It is the first time that GPM *CO* captures a medicane during its mature stage. The main points of this synthesis are provided in the following:

- Based on the available data, Ianos was among the strongest medicanes observed in the Mediterranean in the last at least 25 years. Its central pressure was measured to 984.3 hPa and the wind speed reached 54 m s^{-1} . Daily accumulated rainfall during Ianos exceeded 600 mm in western Greece and 300 mm over parts of central Greece, resulting in four casualties and extensive damage to property and infrastructure caused by floods and landslides.

- Ianos initially developed close to a thunderstorm cluster in the Gulf of Sidra, over a pool of warm sea surface waters on 15 September 2020. Its developing phase lasted more than 48 h and at ~0300 UTC 17 September it became a medicane. Ianos followed a path toward western Greece and finally dissipated over the coasts of Egypt, 7 days after its formation. Its total path over the Mediterranean waters exceeded 1900 km.
- Satellite infrared imagery, as well as lightning data, permitted to follow the convective activity associated with Ianos, from its developing phase, toward its mature stage when convective activity significantly decreased in the outer parts of the cyclone and intense convection was mostly active close to the medicane core. These results provide a different evolution for the distribution and intensity of convection with the three medicanes between 2003 and 2006 that were examined by Claud et al. (2010) and Miglietta et al. (2013), during which deep convection and precipitating clouds were not detected close to the center during the maximum cyclone intensity, despite the impressive cloud-free “eye” formation.
- Analysis of global model fields revealed the upper-level precursors to Ianos development and mainly the role of an upper-tropospheric PV streamer on the intensification of the vortex during the initial stage of Ianos formation.
- High values of EPWAT offshore western Greece as well as over central Greece clearly identified the area where the highest accumulations of rainfall occurred.
- Three GPM *CO* overpasses permitted to follow the cloud and precipitation structures associated with Ianos, during its developing and its mature phase. High-frequency *Tb* revealed details about the precipitation and cloud band evolution of the storm that were not evident in the geostationary imagery. Precipitation radar reflectivity, revealed for the first time the fine structure of cloud bands around a medicane during its mature (or TLC) phase and permitted the identification of certain reflectivity features in the three-dimensional space during Ianos’s mature stage.

Medicanes are rare phenomena but can lead to high impact events in the Mediterranean countries. We believe that such studies contribute to the enrichment of our knowledge and the improvement of our understanding of medicane formation and evolution. Besides the obvious scientific benefits, the increased ability to forecast medicanes and their impacts should be exploited to promote a better societal preparedness and increased coping capacity.

Acknowledgments. The authors acknowledge EUMETSAT for the provision of MSG SEVIRI data, NASA and JAXA for the GPM data, and NCEP, United States, for the provision of FNL model analyses. Both observational and reanalysis datasets will be available upon request.

References

- Buongiorno Nardelli, B., C. Tronconi, A. Pisano, and R. Santoleri, 2013: High and ultra-high resolution processing of satellite sea surface temperature data over southern European seas in the framework of MyOcean project. *Remote Sens. Environ.*, **129**, 1–16, <https://doi.org/10.1016/j.rse.2012.10.012>.
- Cioni, G., P. Malguzzi, and A. Buzzi, 2016: Thermal structure and dynamical precursor of a Mediterranean tropical-like cyclone. *Quart. J. Roy. Meteor. Soc.*, **142**, 1757–1766, <https://doi.org/10.1002/qj.2773>.
- , D. Cerrai, and D. Klocke, 2018: Investigating the predictability of a Mediterranean tropical-like cyclone using a storm-resolving model. *Quart. J. Roy. Meteor. Soc.*, **144**, 1598–1610, <https://doi.org/10.1002/qj.3322>.
- Claud, C., B. Alhammoud, B. M. Funatsu, and J. P. Chaboureaud, 2010: Mediterranean hurricanes: Large-scale environment and convective and precipitating areas from satellite microwave observations. *Nat. Hazards Earth Syst. Sci.*, **10**, 2199–2213, <https://doi.org/10.5194/nhess-10-2199-2010>.
- Dafis, S., J. F. Rysman, C. Claud, and E. Flaounas, 2018: Remote sensing of deep convection within a tropical-like cyclone over the Mediterranean Sea. *Atmos. Sci. Lett.*, **19**, e823, <https://doi.org/10.1002/asl.823>.
- , C. Claud, V. Kotroni, K. Lagouvardos, and J.-F. Rysman, 2020: Insight into convective evolution of Mediterranean tropical-like cyclones. *Quart. J. Roy. Meteor. Soc.*, **146**, 4147–4169, <https://doi.org/10.1002/qj.3896>.
- Draper, D. W., D. A. Newell, F. J. Wentz, S. Krimchansky, and G. M. Skofronick-Jackson, 2015: The Global Precipitation Measurement (GPM) Microwave Imager (GMI): Instrument overview and early on-orbit performance. *IEEE J. Sel. Top. Appl. Earth Obs. Remote Sens.*, **8**, 3452–3462, <https://doi.org/10.1109/JSTARS.2015.2403303>.
- Feidas, H., and A. Giannakos, 2011: Identifying precipitating clouds in Greece using multispectral infrared Meteosat Second Generation satellite data. *Theor. Appl. Climatol.*, **104**, 25–42, <https://doi.org/10.1007/s00704-010-0316-5>.
- Fita, L., and E. Flaounas, 2018: Medicanes as subtropical cyclones: The December 2005 case from the perspective of surface pressure tendency diagnostics and atmospheric water budget. *Quart. J. Roy. Meteor. Soc.*, **144**, 1028–1044, <https://doi.org/10.1002/qj.3273>.
- Flaounas, E., S. L. Gray, and F. Teubler, 2020: A process-based anatomy of Mediterranean cyclones: From baroclinic lows to tropical-like systems. *Wea. Climate Dyn.*, **2**, 255–279, <https://doi.org/10.5194/wcd-2-255-2021>.
- Hou, A. Y., and Coauthors, 2014: The Global Precipitation Measurement mission. *Bull. Amer. Meteor. Soc.*, **95**, 701–722, <https://doi.org/10.1175/BAMS-D-13-00164.1>.
- Kalimeris, A., S. Kolios, D. Halvatzaras, D. Posa, S. Delaco, M. Palma, C. Skordilis, and M. Myrsilides, 2015: The Ionian-Puglia network of meteorological-environmental stations: Geophysical environment and technical description. *Odysseus Tech. Rep.*, 7, 45 pp., <http://ionianweather.gr/en/scientific-articles/ionian-meteorology-and-climatology-en.html>.
- Kojima, M., and Coauthors, 2012: Dual-Frequency Precipitation Radar (DPR) development on the Global Precipitation Measurement (GPM) Core Observatory. *Proc. SPIE*, **8528**, 85281A, <https://doi.org/10.1117/12.976823>.
- Koseki, S., P. A. Mooney, W. Cabos, M. Á. Gaertner, A. de la Vara, and J. J. González Alemán, 2020: Modelling a tropical-like cyclone in the Mediterranean Sea under present and warmer climate. *Nat. Hazards Earth Syst. Sci.*, **21**, 53–71, <https://doi.org/10.5194/nhess-21-53-2021>.
- Kotroni, V., and K. Lagouvardos, 2016: Lightning in the Mediterranean and its relation with sea-surface temperature. *Environ. Res. Lett.*, **11**, 034006, <https://doi.org/10.1088/1748-9326/11/3/034006>.
- Lagouvardos, K., V. Kotroni, S. Nickovic, D. Jovic, G. Kallos, and C. J. Tremback, 1999: Observations and model simulations of a winter sub-synoptic vortex over the central Mediterranean. *Meteor. Appl.*, **6**, 371–383, <https://doi.org/10.1017/S1350482799001309>.
- , and Coauthors, 2017: The automatic weather stations NOANN network of the National Observatory of Athens: Operation and database. *Geosci. Data J.*, **4**, 4–16, <https://doi.org/10.1002/gdj3.44>.
- Marra, A. C., and Coauthors, 2019: The precipitation structure of the Mediterranean tropical-like Cyclone Numa: Analysis of GPM observations and numerical weather prediction model simulations. *Remote Sens.*, **11**, 1690, <https://doi.org/10.3390/rs11141690>.
- Marullo, S., B. Buongiorno Nardelli, M. Guarracino, and R. Santoleri, 2007: Observing the Mediterranean Sea from space: 21 years of Pathfinder-AVHRR sea surface temperatures (1985 to 2005): Re-analysis and validation. *Ocean Sci.*, **3**, 299–310, <https://doi.org/10.5194/os-3-299-2007>.
- Mazza, E., U. Ulbrich, and R. Klein, 2017: The tropical transition of the October 1996 medicane in the western Mediterranean Sea: A warm seclusion event. *Mon. Wea. Rev.*, **145**, 2575–2595, <https://doi.org/10.1175/MWR-D-16-0474.1>.
- Miglietta, M. M., and R. Rotunno, 2019: Development mechanisms for Mediterranean tropical-like cyclones (medicanes). *Quart. J. Roy. Meteor. Soc.*, **145**, 1444–1460, <https://doi.org/10.1002/qj.3503>.
- , S. Laviola, A. Malvaldi, D. Conte, V. Levizzani, and C. Price, 2013: Analysis of tropical-like cyclones over the Mediterranean Sea through a combined modeling and satellite approach. *Geophys. Res. Lett.*, **40**, 2400–2405, <https://doi.org/10.1002/grl.50432>.
- , D. Cerrai, S. Laviola, E. Cattani, and V. Levizzani, 2017: Potential vorticity patterns in Mediterranean “hurricanes.” *Geophys. Res. Lett.*, **44**, 2537–2545, <https://doi.org/10.1002/2017GL072670>.
- Noyelle, R., U. Ulbrich, N. Becker, and E. P. Meredith, 2019: Assessing the impact of sea surface temperatures on a simulated medicane using ensemble simulations. *Nat. Hazards Earth Syst. Sci.*, **19**, 941–955, <https://doi.org/10.5194/nhess-19-941-2019>.
- Olander, T. L., and C. Velden, 2009: Tropical cyclone convection and intensity analysis using differenced infrared and water vapor imagery. *Wea. Forecasting*, **24**, 1558–1572, <https://doi.org/10.1175/2009WAF2222284.1>.
- Picornell, M. A., J. Campins, and A. Jansà, 2014: Detection and thermal description of medicanes from numerical simulation. *Nat. Hazards Earth Syst. Sci.*, **14**, 1059–1070, <https://doi.org/10.5194/nhess-14-1059-2014>.
- Sudradjat, A., R. R. Ferraro, and M. Fiorino, 2005: A comparison of total precipitable water between reanalyses and NVAP. *J. Climate*, **18**, 1790–2007, <https://doi.org/10.1175/JCLI3379.1>.
- Tous, M., and R. Romero, 2013: Meteorological environments associated with medicane development. *Int. J. Climatol.*, **33**, 1–14, <https://doi.org/10.1002/joc.3428>.
- Winstanley, D., 1970: The North African flood disaster, September 1969. *Weather*, **25**, 390–403, <https://doi.org/10.1002/j.1477-8696.1970.tb04128.x>.
- Zekkos, D., and Coauthors, 2020: The September 18–202020 Medicane Ianos impact on Greece—Phase I reconnaissance report. *Geotechnical Extreme Events Reconnaissance Rep.* GEER-068, 198 pp., <https://doi.org/10.18118/G6MT1T>.